Int. J. Heat Mass Transfer. Vol. 32, No. 3, pp. 575–584, 1989
Printed in Great Britain

0017–9310/89 $3.00 + 0.00

Transient conduction in a cylindrical shell with a time-varying incident surface heat flux and convective and radiative surface cooling

BENGT SUNDEN

Department of Applied Thermodynamics and Fluid Mechanics, Chalmers University of Technology, 41296 Göteborg, Sweden

(*Received* 22 *July* 1988 *and in final form* 31 *August* 1988)

Abstract—Numerical calculations based on finite difference approximations are carried out to assess the thermal response of a circular cylindrical shell due to a time-varying incident surface heat flux. The shell is cooled by combined convection and thermal radiation. Temperature distributions vs time and space (in non-dimensional form) are provided and the influence of the leading physical parameters (Biot, radiation, heat flux and Fourier numbers) is presented. For a poorly heat conducting shell material, the maximum temperature is high if efficient cooling by convection and radiation is not maintained.

INTRODUCTION

COMBINED modes of heat transfer occur in many problems of engineering interest. For instance, transient heat conduction in a solid with convective and/or radiative cooling at the surfaces of the solid occurs frequently. In the past, a number of papers on this subject were published. During recent years a few papers have appeared.

Crosbie and Viskanta [1] presented a study of transient cooling and heating of a plate by combined convection and radiation. The transient heat conduction equation and the boundary conditions were transformed to a non-linear Volterra integral equation of the second kind for the surface temperature. This equation was solved numerically by the method of successive approximations. A review of earlier studies was also given.

Davies [2] employed a one-dimensional approximate solution method in analysing the transient heat conduction in a plate heated by convection and cooled by radiation.

In refs. [3, 4] studies of transient heat conduction in various composite slabs heated by a time-varying incident heat flux and cooled by combined convection and radiation were presented. The slabs were also rotating with constant speeds. An implicit finite difference technique was used in the numerical calculations.

Tsai and Nixon [5] analysed a problem similar to those in refs. [3, 4] but also included thermal radiation within the solid as well as internal heat generation. The incident heat flux was constant in time and the slab was not rotating. A hybrid numerical algorithm with a Runge–Kutta technique for the time variable and a finite difference method for the space variable was employed.

This paper is concerned with the unsteady heat conduction in a solid cylindrical shell which is exposed to a time-varying incident heat flux such as a nuclear thermal pulse. The outer surface of the solid is cooled by convection and radiation. The heat conduction is taken as two-dimensional in space and the inner surface of the shell is insulated. The problem originates from a real world application. The main objective of this paper is to predict the temperature distribution in the solid shell as a function of time and space, and to predict the peak temperatures. The details of the numerical method are described briefly.

Heat transfer problems related to the one to be presented, besides those already cited, are found for space vehicles and satellites exposed to solar radiation. In free space, convective heat transfer is negligible and thus only conduction in the solid material and radiation at its surfaces are considered. Nichols [6] calculated surface temperature distributions in thin-walled spheres, cylinders and cones subjected to solar radiation. Rotation of these bodies was also considered. Only the surface temperature distributions were analysed and the equations were solved numerically. In refs. [7–9] analytical solutions of the temperature distribution in thin-walled rotating cylindrical and spherical bodies were presented. The non-linear boundary condition was approximated to a linear form. A similar solution for a thick-walled spherical satellite was given by Prelewicz and Kennedy [10]. Steady-state solutions of the heat conduction equation for spherical and cylindrical bodies subjected to solar heating have been presented in refs. [11–13].

The study most relevant to this paper is that of Olmstead *et al.* [9]. Besides heating by the sun, heating of a cylindrical shell by a time-dependent incident heat flux, corresponding to a nuclear thermal pulse, was studied. However, only conduction in the circumferential direction was considered and no convective heat loss was present. Parametric variations

NOMENCLATURE

a_1	thermal diffusivity, $k/\rho c_p$
$a_{i,j}, b_{i,j}, c_{i,j}, d_{i,j}$	coefficients in the numerical solution
Bi	Biot number, $h(r_2-r_1)/k$
c_1	$r_1/(r_2-r_1)$
c_p	specific heat
HN	heat flux number, $\alpha\dot{Q}_{\max}(r_2-r_1)/kT_i$
h	convective heat transfer coefficient
i,j	integers
k	thermal conductivity
M	radiation number, $\sigma\varepsilon T_i^3(r_2-r_1)/k$
n	time level
$\dot{Q}$	incident heat flux
$\dot{Q}_{\max}$	maximum value of $\dot{Q}$
R'	$r'+c_1$
r	radial coordinate
r_1	inner radius of the solid shell
r_2	outer radius of the solid shell
r'	dimensionless radial coordinate, $(r-r_1)/(r_2-r_1)$
$\Delta r'$	dimensionless step size in the radial direction
T	temperature
T_i	initial temperature
T_{01}	radiation background temperature
T_{02}	ambient air temperature
T_s	surface temperature
T'	dimensionless temperature, $(T-T_i)/T_i$
T'_{01}	dimensionless radiation background temperature
T'_{02}	dimensionless ambient air temperature
T'_s	dimensionless surface temperature
t	time
t'	Fourier number, $a_1 t/(r_2-r_1)^2$
$\Delta t'$	time increment [nondimensional].

Greek symbols

α	absorptivity for the incident radiative heat flux
γ	angle
ε	emissivity for thermal radiation
θ	angle coordinate
ρ	density
σ	Stefan–Boltzmann constant
φ	dimensionless angle, θ/π
$\Delta\varphi$	dimensionless step size in the circumferential direction.

were not considered either. Thus the present paper will provide new and additional results.

It also should be noted that in handbooks, e.g. ref. [14], several examples of transient conduction with various surface conditions are available but unfortunately they are not applicable to the case which is considered in this paper.

STATEMENT OF PROBLEM

Consider a circular cylindrical solid shell as shown in Fig. 1. Initially the solid has a uniform temperature T_i and suddenly its outer front surface is exposed to a high incident radiative heat flux which is varying in time as depicted in Fig. 2. The incident surface heat flux can in this case be regarded as an optically parallel beam and thus at every position on the front surface, the heat flux has to be multiplied by the cosine of the angle between the surface normal and the direction of the incident heat flux. The rear surface of the solid is not exposed to the incident heat flux. The outer surface (both front and rear parts) of the solid exchanges heat with the surrounding environment by convection and radiation. The inner surface is in direct contact with a centrebody. This centrebody has such a low thermal conductivity that the inner surface can be regarded as insulated at every instant of time. The conduction in the solid shell is assumed to be two-dimensional and the coordinate system is placed as shown in Fig. 1. The solid is assumed to be opaque to thermal radiation and no internal heat sources or heat sinks are present. The physical properties are uniform and independent of temperature and the convective heat transfer coefficient is considered to be independent of the outer surface temperature. The ambient air is transparent to thermal radiation and its temperature T_{02} is independent of time. The background radiation temperature is constant and denoted by T_{01}.

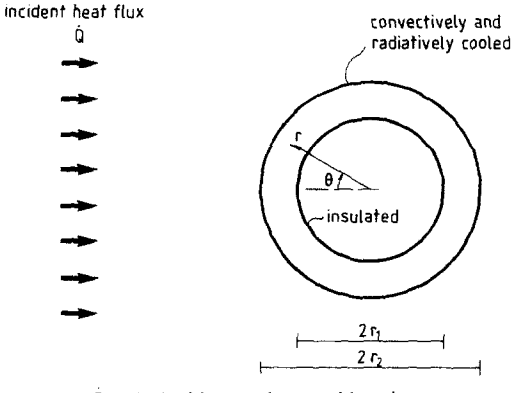

FIG. 1. Problem under consideration.

GOVERNING EQUATIONS AND BOUNDARY CONDITIONS

The two-dimensional form of the heat conduction equation in cylindrical polar coordinates yields

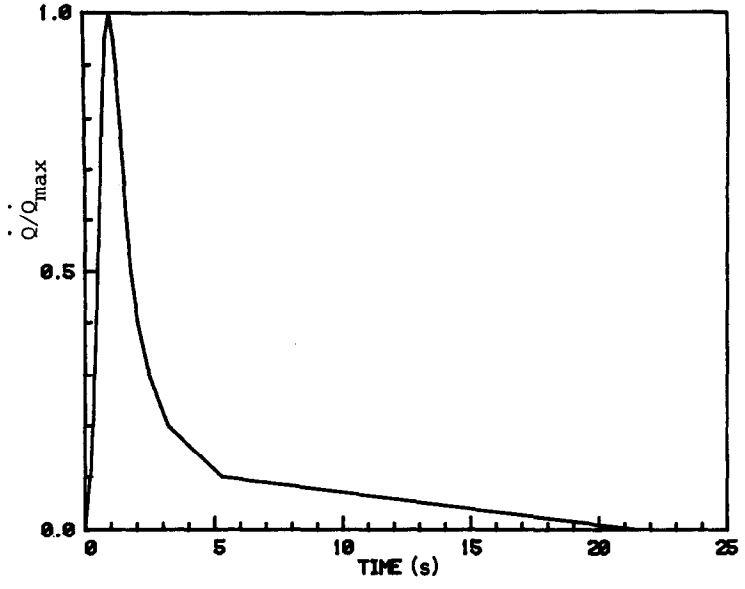

FIG. 2. Incident heat flux vs time.

$$\frac{\partial T}{\partial t} = a_1\left(\frac{\partial^2 T}{\partial r^2} + \frac{1}{r}\frac{\partial T}{\partial r} + \frac{1}{r^2}\frac{\partial^2 T}{\partial \theta^2}\right) \tag{1}$$

where a_1 is the thermal diffusivity of the solid shell. This equation is cast into a non-dimensional form by introducing the following variables:

$$T' = (T-T_i)/T_i, \quad r' = (r-r_1)/(r_2-r_1)$$
$$\varphi = \theta/\pi, \quad t' = a_1 t/(r_2-r_1)^2. \tag{2}$$

One then has

$$\frac{\partial T'}{\partial t'} = \frac{\partial^2 T'}{\partial r'^2} + \frac{1}{r'+c_1}\frac{\partial T'}{\partial r'} + \frac{1}{\pi^2(r'+c_1)^2}\frac{\partial^2 T'}{\partial \varphi^2} \tag{3}$$

where

$$c_1 = r_1/(r_2-r_1).$$

Initially, the solid is at a uniform temperature. The initial condition is expressed as

$$T'(r', \varphi, 0) = 0. \tag{4}$$

The inner surface is assumed to be insulated and the boundary condition to be

$$\frac{\partial T'}{\partial r'}(0, \varphi, t') = 0. \tag{5}$$

For the outer surface, exposed to the incident radiative heat flux, a heat balance implies:

absorbed incident heat flux − thermal radiation loss

− convective cooling − outward conduction = 0.

In mathematical terms and with the non-dimensional variables this condition reads

$$\frac{(r_2-r_1)\alpha\dot{Q}\cos(\gamma)}{kT_i} - \frac{(r_2-r_1)\sigma\varepsilon T_i^3((T'_s+1)^4-(T'_{01}+1)^4)}{k} - \frac{(r_2-r_1)h}{k}(T'_s-T'_{02}) - \frac{\partial T'}{\partial r'} = 0 \tag{6}$$

where γ is the angle between the surface normal and the direction of the incident parallel beam of radiant energy, T'_{01} and T'_{02} the dimensionless temperatures of the background radiation and the surrounding air, respectively, and T'_s is the dimensionless surface temperature $T'(1, \varphi, t')$. k is the thermal conductivity of the solid and h the convective heat transfer coefficient.

In equation (6), two important and well-known non-dimensional numbers are identified, i.e. the Biot number $Bi = h(r_2-r_1)/k$ and the radiation number $M = \sigma\varepsilon T_i^3(r_2-r_1)/k$. Also the group $\alpha\dot{Q}(r_2-r_1)/kT_i$ presents a non-dimensional number but it varies with time. A heat flux number $HN = \alpha\dot{Q}_{max}(r_2-r_1)/kT_i$ is defined here to represent the incident heat flux.

The convective heat transfer coefficient h is known to vary with the circumferential position for forced as well as natural convection. In engineering calculations, an average value of the heat transfer coefficient is usually used and in this paper an average value is mainly applied. Various values of h are covered by varying the Biot number. However, the effect of a non-uniform heat transfer coefficient around the exposed shell will be presented.

The importance of the radiative and convective cooling can be studied by using various values of the

radiation number M and the Biot number Bi while the strength of the heat flux is controlled by the heat flux number HN. When generalizing the results, one has to remember that the variation of the incident heat flux is given as a function of real time. This means that for solids having different thermal diffusivities the order of magnitude of the Fourier number Fo may differ considerably. Also, since the thermal conductivity appears in the dimensionless numbers Bi, M and HN, a solid with a high thermal conductivity corresponds to smaller values of Bi, M and HN than for a poor heat conducting solid at the same magnitude of the incident heat flux and convective heat transfer coefficient.

METHOD OF NUMERICAL SOLUTION

Equation (3) is solved numerically by using finite difference approximations. The symmetry is taken into account and the solution domain is bounded by $\varphi = 0$ and 1. In the space coordinates central second-order approximations are employed while for the discretization in time a first-order approximation is used.

The derivatives in equations (5) and (6) are calculated by second-order forward and backward finite difference approximations, respectively.

Due to the non-linear boundary condition, equation (6), the equations are solved iteratively at each time level.

With the finite difference approximations introduced, equation (3) can be written in the form (i, circumferential direction; j, radial direction)

$$a_{i,j}T'^{n+1}_{i,j} = b_{i,j}T'^{n+1}_{i,j+1} + c_{i,j}T'^{n+1}_{i,j-1} + d_{i,j} \tag{7}$$

where

$$a_{i,j} = \frac{1}{\Delta t'} + \frac{2}{\Delta r'^2} + \frac{2}{R'^2\pi^2\Delta\varphi^2} \tag{8}$$

$$b_{i,j} = 1/(\Delta r'^2) + 1/(2R'\Delta r') \tag{9}$$

$$c_{i,j} = 1/(\Delta r'^2) - 1/(2R'\Delta r') \tag{10}$$

$$d_{i,j} = T'^{n}_{i,j}/\Delta t' + (T'^{n}_{i+1,j} + T'^{n+1}_{i-1,j})/(\pi^2 R'^2 \Delta\varphi^2). \tag{11}$$

In equations (7) and (11) n denotes the time level and $R' = r' + c_1$.

From equations (7) and (11) it is obvious that a fully implicit formulation is used in the radial direction while in the circumferential direction the formulation is explicit.

The solution procedure starts at $\varphi = 0$ and proceeds sector by sector to $\varphi = 1$. First the outer surface temperature is calculated from equation (6). Then equation (7) is solved by using the TDMA algorithm. When $\varphi = 1$ has been reached, the procedure restarts at $\varphi = 0$ (the boundary conditions at $\varphi = 0$ and 1 are updated) and continues until the convergence criterion is satisfied. In this case, the convergence criterion in the iterative solution procedure was set on the outer surface temperature. When the relative change in all surface temperatures, between successive iterations, was less than 10^{-4} the solution was considered to have converged.

Sample calculations

The parameters for the present problem are: the Fourier number Fo, the radiation number M, the Biot number Bi, the heat flux number HN and the size of the shell. As was stated previously, the incident heat flux is given as a function of real time (Fig. 2). This means that the magnitude of the Fourier number (corresponding to this time period) will depend on the thermal diffusivity of the shell material. In this paper, two different materials are considered, one poorly conducting (low thermal diffusivity) and the other highly conducting (high thermal diffusivity). The size of the shell will be kept constant while the other parameters are permitted to vary arbitrarily.

The appropriate number of grid points in the space plane was determined by test calculations of some corresponding steady-state problems. For the particular size of the shell ($r_1 = 5.9$ mm, $r_2 = 7.3$ mm), it was found that 21 grid points in the radial direction ($\Delta r' =$ constant) and 32 grid points in the circumferential direction ($\Delta\varphi =$ constant) gave sufficient accuracy. For another shell size the necessary number of grid points may differ.

The time step $\Delta t'$ was determined by considering the time scale of the shell material and the time dependence of the incident radiative heat flux. Test calculations showed that for a shell material having a thermal diffusivity $a_1 = 6.6 \times 10^{-8}$ m^2 s^{-1}, the proper non-dimensional time step was 3.4×10^{-5} (real time 0.001 s) while if $a_1 = 6.5 \times 10^{-5}$ a dimensionless time step of 3.3×10^{-3} (real time 0.0001 s) was sufficient. For the time periods covered in the final calculations, 4000 and 20 000 time steps, respectively, were used.

The ambient air temperature is equal to the initial temperature and thus $T'_{02} = 0$. The background radiation temperature is in the real world application 283 K and the initial temperature is 298 K. Thus the dimensionless temperature $T'_{01} = -0.05$.

RESULTS AND DISCUSSION

Case 1

The first case corresponds to a shell having a thermal diffusivity $a_1 = 6.6 \times 10^{-8}$ m^2 s^{-1}. The heat flux number HN corresponding to the maximum value of the incident heat flux is 8.8.

Figure 3 shows the dimensionless temperature at $\varphi = 0$ vs the dimensionless time (Fourier number) for various combinations of Bi and M. For the case with $Bi = M = 0$ no cooling of the shell occurs. The surface temperature starts to increase rapidly, reaches a maximum and then begins to decrease as the incident heat flux decays. The decrease in the surface temperature is caused by redistribution within the shell due to heat conduction. This fact can also be seen in Fig. 4 where temperature distributions in the radial direction at $\varphi = 0$ are given at various instants of

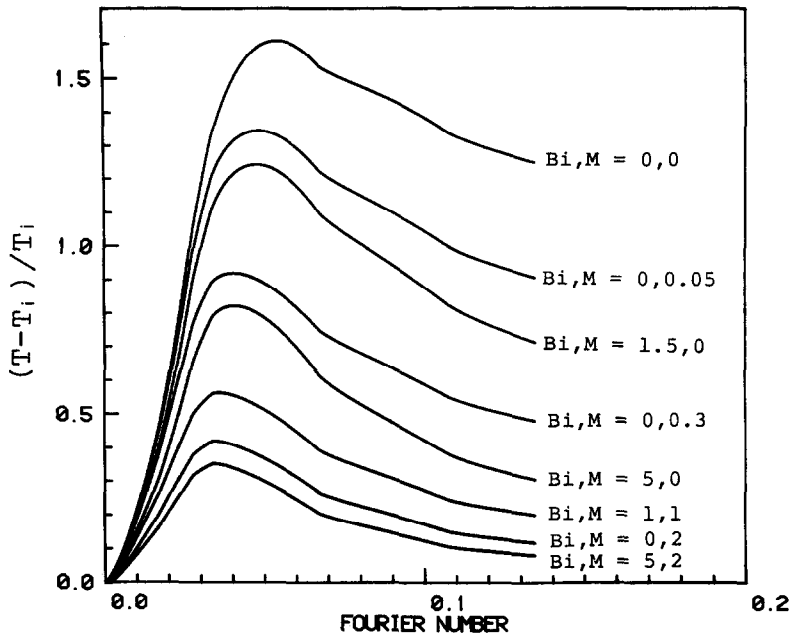

FIG. 3. Influence of the Biot (Bi) and radiation (M) numbers on the non-dimensional surface temperature at $\varphi = 0$. Case 1, $HN = 8.8$.

time. As time proceeds the heat penetrates deeper and deeper into the shell.

As Bi and M are increased, the cooling of the shell is enhanced and as an effect the maximum temperature becomes lower (Fig. 3). The rate of increase in temperature during the heating up phase is smaller and the decrease, after the maximum temperature has been reached, is faster as cooling of the surface now occurs. The instant of time at which the maximum temperature occurs is also affected by Bi and M. Generally, as the values of Bi and M are increased, the maximum temperature is reached earlier. From the results in Fig. 3, it is obvious that to create an identical cooling effect, the radiation number can be less than the Biot number Bi.

Figure 4 also shows temperature distributions in the radial direction for $Bi = M = 1$ at those Fourier numbers which were displayed for $Bi = M = 0$. Also

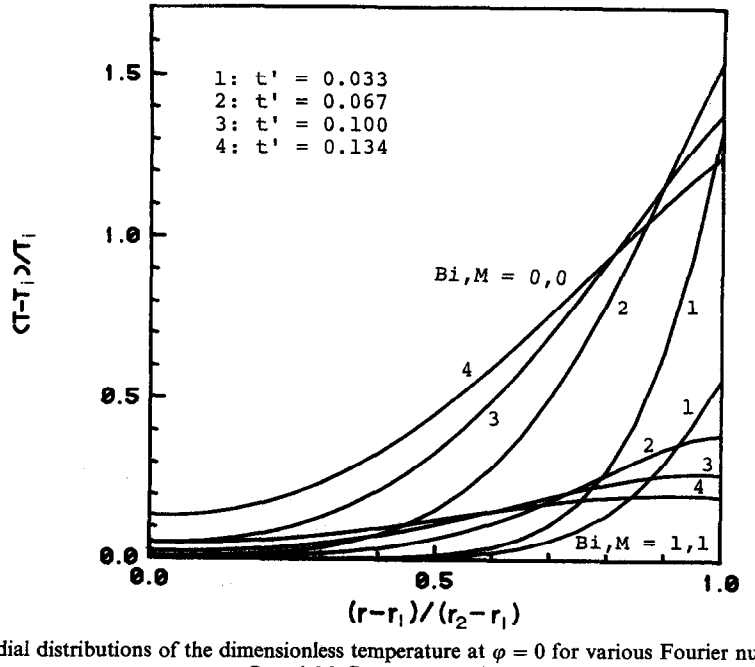

FIG. 4. Radial distributions of the dimensionless temperature at $\varphi = 0$ for various Fourier numbers (t'), Bi and M. Case 1, $HN = 8.8$.

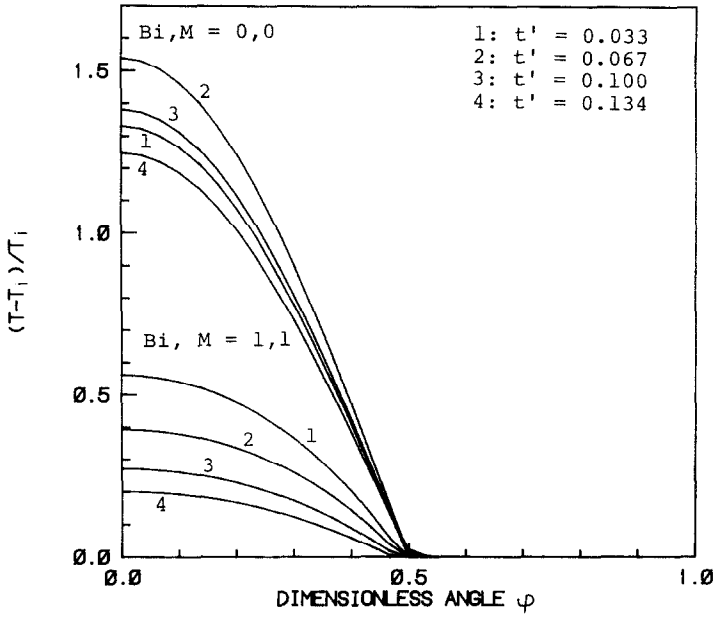

FIG. 5. Circumferential variations of the surface temperature $T'(1, \varphi, t')$. Case 1, $HN = 8.8$.

here redistribution of the temperature due to heat conduction occurs but the surface temperature decreases monotonically with increasing Fourier number contrary to the results for $Bi = M = 0$.

The circumferential variations of the surface temperature $T'(1, \varphi, t')$ are depicted in Fig. 5. The rear part of the shell remains at the initial temperature over the time period considered. This is so because the heat conduction in the circumferential direction is poor and no incident heat flux occurs on the rear side of the shell. Again the influence of Bi and M on the time dependence is obvious. For $Bi = M = 0$, strong variations along the surface exist while for $Bi = M = 1$ relatively weak variations occur.

Temperature distributions similar to those in Fig. 4 show up at any angular position on the front side of the shell. The temperature levels are lower in agreement with Fig. 5.

Varying heat transfer coefficient

For all the values of Bi and M used in this study, the rear side of the cylindrical shell remains at the initial temperature. A circumferential variation of the heat transfer coefficient on the rear side will thus not change the temperature distributions in Figs. 3–5.

To show the effect of a varying heat transfer coefficient on the front side the following cases are compared in Fig. 6: (a) $Bi = 1$ (uniform), $M = 1$ already shown in Figs. 3–5; (b) $Bi = \cos \pi\varphi$, $0 \leqslant \varphi \leqslant 1/2$, $Bi = 0$, $1/2 \leqslant \varphi \leqslant 1$, $M = 1$. This variation is stronger than that occurring in reality. As is evident, the dimensionless temperatures are slightly higher for case (b), since the convective cooling is poorer. However, the magnitude of the incident heat flux also decreases as φ increases and thus the importance of the heat transfer coefficient is diminished and is not that strong.

Influence of the heat flux number HN

By comparing the non-dimensional temperature distributions for various values of the heat flux number HN, the influence of the magnitude of the incident heat flux and the surface absorptivity can be revealed.

Figure 7 provides non-dimensional temperature distributions vs the Fourier number at $\varphi = 0$ for $HN = 8.8$, 5 and 2. The cooling by convection and radiation is given by $Bi = 1$ and $M = 1$, respectively. The principal behaviour of these distributions is similar but the rate of the temperature increase (before reaching the maximum temperature) is diminished as HN is decreased. Also the maximum temperature at $HN = 2$ is much less than that at $HN = 8.8$. The rate of decrease in temperature, after the maximum temperature has been passed, is also diminished as the heat flux number is decreased.

Distributions of the non-dimensional temperature in the radial and circumferential directions are for all values of HN similar to those shown in Figs. 4 and 5 but the levels differ in agreement with Fig. 7.

Case 2

The second case corresponds to a shell having a thermal diffusivity $a_1 = 6.5 \times 10^{-5}$ m^2 s^{-1}. The heat flux number HN is then 0.0077.

For this particular case, with a high thermal conductivity of the shell material, the relevant values of Bi and M are zero. Thus only the case $Bi = 0$ and $M = 0$ is considered here.

Figure 8 shows the non-dimensional surface temperature at $\varphi = 0$ as a function of the Fourier number.

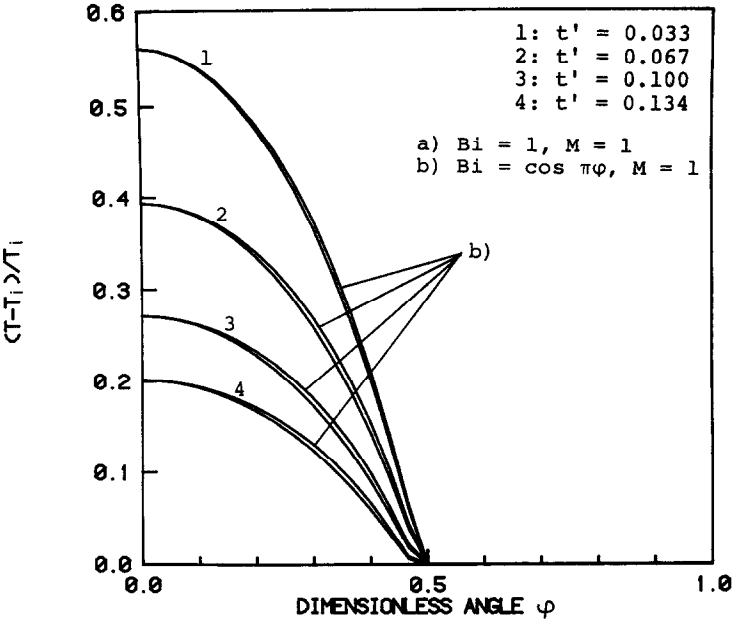

FIG. 6. Influence of circumferentially varying *Bi* (heat transfer coefficient) on the dimensionless temperature distributions. Case 1, $HN = 8.8$: (a) unmarked lines.

Compared to Fig. 3 the striking features are the much lower maximum temperature level and the much higher magnitude of the Fourier number. The temperature starts to increase slowly, reaches a maximum and remains at this level for a long time and then finally starts to decrease slowly (not shown). This decrease is caused by heat conduction in the circumferential direction since no cooling by convection and radiation appears.

In Fig. 9, it can be seen that the temperature is almost uniform in the radial direction due to the high thermal conductivity of this material. This also implies

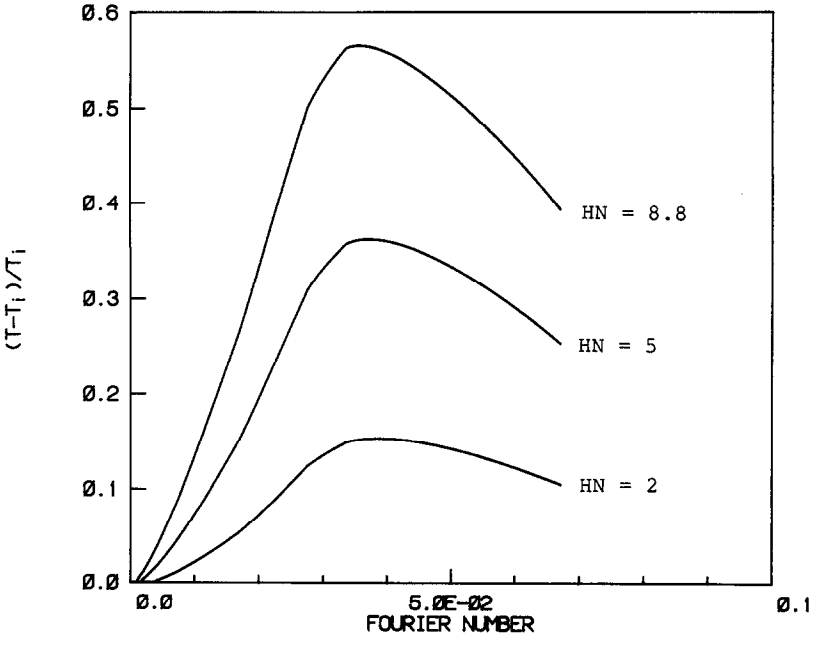

FIG. 7. Influence of the heat flux number *HN* on the non-dimensional surface temperature at $\varphi = 0$. Case 1, $Bi = 1$, $M = 1$.

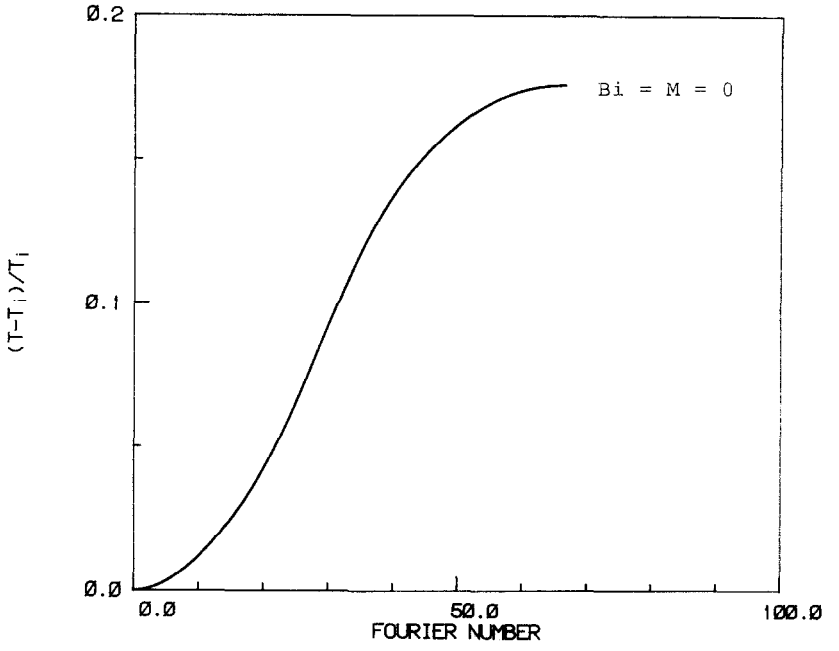

FIG. 8. Non-dimensional surface temperature distribution at $\varphi = 0$. Case 2, $HN = 0.0077$.

that the numerical analysis can be simplified to a one-dimensional one in space.

Figure 10 provides temperature distributions in the circumferential direction. Due to the good heat conduction within the shell material, heat is also transferred to the rear side and the temperatures are increasing gradually with time.

CONCLUSIONS

A numerical investigation of the transient conduction in a cylindrical shell exposed to a time-varying incident surface heat flux has been performed.

The importance of the convective and radiative cooling of the shell surface has been revealed. For a

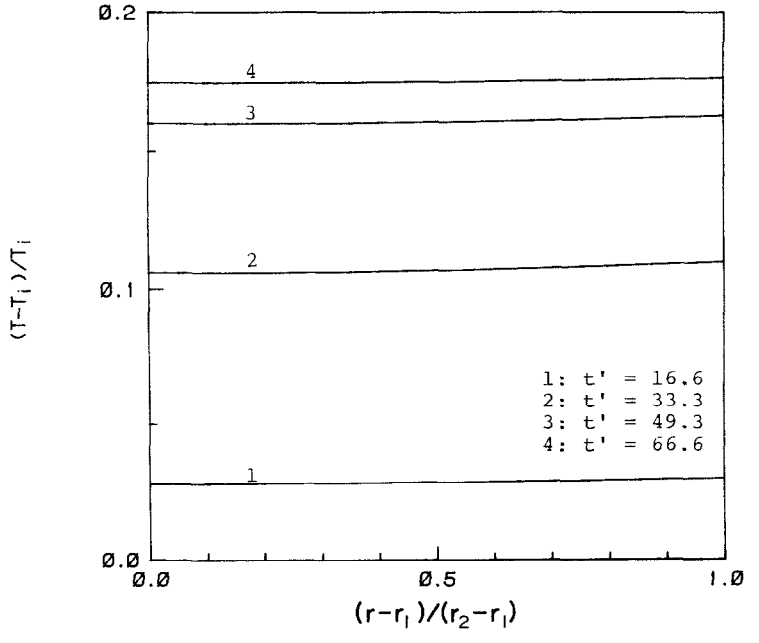

FIG. 9. Radial distributions of the dimensionless temperature at $\varphi = 0$ for various Fourier numbers (t'). Case 2, $HN = 0.0077$.

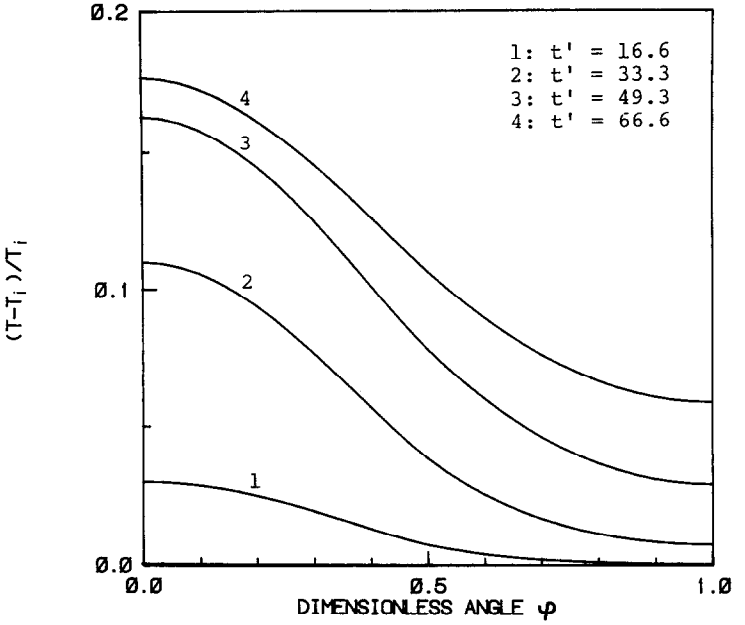

FIG. 10. Circumferential variation of the surface temperature $T'(1, \varphi, t')$. Case 2, $HN = 0.0077$.

shell material with a low thermal conductivity (and low thermal diffusivity) the effect of increasing the Biot and the radiation numbers is strong. It seems that the rate of cooling by thermal radiation is most essential.

For a shell material with a high thermal conductivity (and a high thermal diffusivity), the temperature levels are much lower and the temperature distributions are uniform in the radial direction. Heat is also transferred (by conduction) to the unexposed rear side of the shell which is not the case for a poorly conducting shell material.

REFERENCES

1. A. L. Crosbie and R. Viskanta, Transient heating or cooling of a plate by combined convection and radiation, *Int. J. Heat Mass Transfer* **11**, 305–317 (1968).
2. T. W. Davies, Transient conduction in a plate with counteracting convection and thermal radiation at the boundaries, *Appl. Math. Modelling* **9**, 337–340 (1985).
3. B. Sunden, Transient heat conduction in a composite slab by a time-varying incident heat flux combined with convective and radiative cooling, *Int. Commun. Heat Mass Transfer* **13**, 515–522 (1986).
4. B. Sunden, Numerical prediction of transient heat conduction in a multilayered solid with time-varying surface conditions. In *Numerical Methods in Thermal Problems*, Vol. V, pp. 207–218. Pineridge Press, Swansea (1987).
5. C. F. Tsai and G. Nixon, Transient temperature distribution of a multilayer composite wall with effects of internal thermal radiation and conduction, *Numer. Heat Transfer* **10**, 95–101 (1986).
6. L. D. Nichols, Surface temperature distribution on thin-walled bodies subjected to solar radiation in interplanetary space, NACA TN D-584 (1961).
7. A. Charnes and S. Raynor, Solar heating of a rotating cylindrical space vehicle, *ARS J.* **30**(5), 479–484 (1960).
8. W. E. Olmstead and S. Raynor, Solar heating of a rotating spherical space vehicle, *Int. J. Heat Mass Transfer* **5**, 1165–1177 (1962).
9. W. E. Olmstead, L. A. Peralta and S. Raynor, Transient radiation heating of a rotating cylindrical shell, *AIAA J.* **1**(9), 2166–2168 (1963).
10. D. A. Prelewicz and L. A. Kennedy, Radiant heating of a rotating thick-walled spherical satellite, *AIAA J.* **5**(1), 179–181 (1967).
11. M. Iqbal and B. D. Aggarwala, Solar heating of a long circular cylinder with semigray surface properties, *J. Spacecraft* **5**(10), 1229–1231 (1968).
12. M. Iqbal and B. D. Aggarwala, Radiant heating of a solid spherical satellite, *AIAA J.* **7**(4), 784–786 (1969).
13. S. Sikka, M. Iqbal and B. D. Aggarwala, Temperature distribution and curvature produced in long solid cylinders in space, *J. Spacecraft* **6**(8), 911–916 (1969).
14. P. J. Schneider, Conduction. In *Handbook of Heat Transfer* (Edited by W. M. Rohsenow and J. P. Hartnett), Section 3. McGraw-Hill, New York (1973).

CONDUCTION VARIABLE DANS UNE COQUE CYLINDRIQUE AVEC UN FLUX THERMIQUE SURFACIQUE VARIABLE DANS LE TEMPS ET UNE FACE SE REFROIDISSANT PAR CONVECTION ET RAYONNEMENT

Résumé—Des calculs numériques basés sur des approximations par différences finies sont conduits pour connaitre la réponse thermique d'une coque cylindrique circulaire due à un flux de chaleur pariétal incident qui dépend du temps. La coque est refroidie par une convection liée à du rayonnement. On obtient des distributions de température en fonction du temps et de l'espace (forme adimensionnelle) et on présente l'influence des paramètres adimensionnels physiques (Biot, rayonnement, propriétés conductives du matériau, flux de chaleur et nombre de Fourier). Pour un matériau mauvais conducteur thermique, la température maximale est élevée si le refroidissement par convection et rayonnement n'est pas efficace.

INSTATIONÄRE WÄRMELEITUNG IN EINER ZYLINDRISCHEN SCHALE MIT ZEITABHÄNGIGEM WÄRMESTROM AN DER OBERFLÄCHE BEI KONVEKTION UND STRAHLUNGSKÜHLUNG

Zusammenfassung—Mit der Finite-Differenzen-Methode werden Berechnungen durchgeführt, um die thermische Antwort (Reaktion) eines zeitlich veränderlichen Wärmestroms an der Oberfläche einer kreiszylindrischen Schale zu ermitteln. Die Schale wird dabei durch Konvektion und Strahlung gekühlt. Es ergeben sich zeitliche und örtliche Temperaturverteilungen in dimensionsloser Form. Der Einfluß wichtiger physikalischer Parameter (wie Wärmestrom-, Strahlungs-, Biot- und Fourier-Zahl) wird dargestellt. Für schlecht wärmeleitendes Material ist die maximale Temperatur hoch, wenn keine ausreichende Kühlung durch Konvektion und Strahlung gewährleistet ist.

НЕСТАЦИОНАРНАЯ ТЕПЛОПРОВОДНОСТЬ ЦИЛИНДРИЧЕСКОЙ ОБОЛОЧКИ ПРИ ИЗМЕНЯЮЩЕМСЯ ВО ВРЕМЕНИ ТЕПЛОВОМ ПОТОКЕ К ПОВЕРХНОСТИ И КОНВЕКТИВНОМ И ЛУЧИСТОМ ЕЕ ОХЛАЖДЕНИИ

Аннотация—Для оценки изменения во времени тепловых характеристик круглой цилиндрической оболочки при подводе к ее поверхности теплового потока проведены расчеты на основе конечно-разностных аппроксимаций. Оболочка охлаждается за счет совместного действия конвекции и теплового излучения. Представлены временная и пространственная зависимости изменения температуры (в безразмерном виде), а также роль основных физических параметров (числа Био, излучения, теплового потока и числа Фурье). В случае плохороводящего материала максимальное значение температуры оболочки повышается из-за неэффективного охлаждения конвекцией и излучением.